INSTITUTE FOR NUCLEAR STUDY
UNIVERSITY OF TOKYO
Tanashi, Tokyo 188
Japan

INS-Rep.-711
Oct. 1988

EXPERIMENTAL STUDY OF ^{20}Na AND BREAKOUT OFF THE HOT-CNO CYCLE*

S. Kubono, N. Ikeda, M. Yasue, T. Nomura, Y. Fuchi, H. Kawashima,

S. Kato[1], H. Orihara[2], T. Niizeki[2], S. Hirasaki[2], G. C. Jon[2], T. Shinozuka[2],

H. Ohnuma[3], H. Miyatake[4], T. Shimoda[4], K. Miura[5], and T. Kajino[6]

Institute for Nuclear Study, University of Tokyo, Tanashi, Tokyo, 188 Japan.
1) College of General Education, Yamagata University, Yamagata, 990 Japan.
2) Cyclotron-RI Center, Tohoku University, Sendai, 980 Japan.
3) Department of Physics, Tokyo Institute of Technology, Meguro, Tokyo, 152 Japan.
4) College of General Education, Osaka University, Toyonaka, Osaka, 560 Japan.
5) Tohoku Institute of Technology, Nagamachi, Sendai, 982 Japan.
6) Department of Physics, Tokyo Metropolitan University, Setagaya, Tokyo, 158 Japan.

* Invited paper presented at the International Symposium on Heavy Ion Physics and Nuclear Astrophysical Problems, July 21-23, 1988, Tokyo.

INS-Rep.-711
Oct. 1988

EXPERIMENTAL STUDY OF ^{20}Na AND BREAKOUT OFF THE HOT-CNO CYCLE*

S. Kubono, N. Ikeda, M. Yasue, T. Nomura, Y. Fuchi, H. Kawashima,

S. Kato[1], H. Orihara[2], T. Niizeki[2], S. Hirasaki[2], G. C. Jon[2], T. Shinozuka[2],

H. Ohnuma[3], H. Miyatake[4], T. Shimoda[4], K. Miura[5], and T. Kajino[6]

Institute for Nuclear Study, University of Tokyo, Tanashi, Tokyo, 188 Japan.
1) College of General Education, Yamagata University, Yamagata, 990 Japan.
2) Cyclotron-RI Center, Tohoku University, Sendai, 980 Japan.
3) Department of Physics, Tokyo Institute of Technology, Meguro, Tokyo, 152 Japan.
4) College of General Education, Osaka University, Toyonaka, Osaka, 560 Japan.
5) Tohoku Institute of Technology, Nagamachi, Sendai, 982 Japan.
6) Department of Physics, Tokyo Metropolitan University, Setagaya, Tokyo, 158 Japan.

ABSTRACT

The nuclear levels above the p + ^{19}Ne threshold in ^{20}Na, which are critical for the breakout problem from the hot CNO cycle and the following heavy-element synthesis, have been extensively studied by the (^{3}He,t) and (p,n) reactions on ^{20}Ne. Several new spin-parity assignments have been made. Specifically, the first excited state above the threshold has been identified to be 1^{+} at 2.637 MeV (0.438 MeV above the threshold), indicating this state to be the s-wave resonant state in the p + ^{19}Ne scattering. The stellar reaction rate of the ^{19}Ne(p,γ) process is evaluated for the first time based on the experimental results of ^{20}Na, and the result is more than two orders of magnitude larger than the previous theoretical predictions. The onset temperature of the flow-out from the hot CNO cycle to heavier elements is estimated to be as low as about 2.3 x 10^{8} K, suggesting that the flow-out via this process is an explanation for the strong enhancement in Ne and heavier elements in nova observations.

* Invited paper presented at the International Symposium on Heavy Ion Physics and Nuclear Astrophysical Problems, July 21-23, 1988, Tokyo.

I. INTRODUCTION

Composition of nuclides in the stars and the mechanism of nucleosyntheses is a stringent clew in understanding the stellar evolutions. In explosive hydrogen burning, rapid-proton (rp) process, proposed by Wallace and Woosley[1], will give a chance of breakout from the hot CNO (HCNO) cycle at a certain temperature, and lead to synthesis of heavier elements. Figure 1 depicts the process of the breakout from the HCNO cycle. A strong enhancement in Ne and heavier elements in nova observation has not been explained[2], which awaits elaborate works for the breakout problem from the CNO cycle. Specifically, the capture process of $p + {}^{19}Ne \rightarrow {}^{20}Na$ is crucial for this breakout[1,2,3]. The question here is whether the capture rate at stellar energies is faster than the β-decay rate of ${}^{19}Ne(\beta^+ \nu){}^{19}F$ which eventually goes back to the HCNO cycle via the ${}^{19}F(p,\alpha)$ reaction. However, the nuclear structure information on ${}^{20}Na$ was very scarce[4], especially about the spin-parities of the states above the $p + {}^{19}Ne$ threshold.

Wallace and Woosley[1] estimated the stellar capture rate using the data of the mirror nucleus ${}^{20}F$. This process was recently reevaluated theoretically by Langanke et al.[3] including Thomas-Ehrman shift for estimating the levels of ${}^{20}Na$ and the direct capture contributions. They pointed out that s-wave resonant state (the analogue state in ${}^{20}F$ is the 3.488 MeV 1^+ state) would come down considerably in energy and as a result the stellar reaction rate calculated show a significant increase.

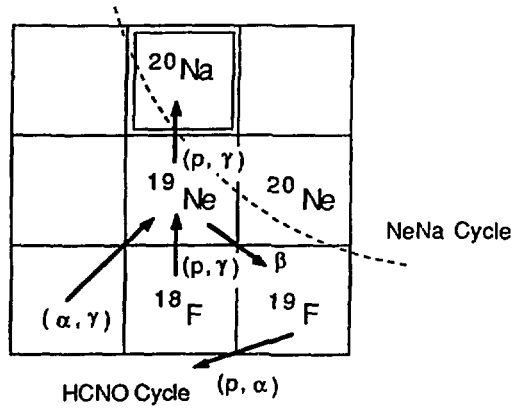

Fig. 1 The flow diagram of the breakout off the HCNO cycle.

Until very recently there were very few experimental works reported. Only two broad states were known above the threshold in ^{20}Na. Aysto et al.[5] have studied β-delayed particle decays of ^{20}Na and found proton decay states at 6.15 and 6.36 MeV. However, the states near the p + ^{19}Ne threshold were not studied. The broad peak at 2.9 MeV was recently separated into some states by Lamm et al.[6]. However, no spin assignment was made for the states.

We report here the experimental results of the (^{3}He,t) and (p,n) reactions on ^{20}Ne and several new spin-parity assignments for the states just above the threshold including s-wave resonant state[7] of p + ^{19}Ne, the evaluation of the stellar reaction rate of the ^{19}Ne(p,γ) process based on the present experimental data, and the onset temperature of the breakout from the HCNO cycle. The experimental details are described in sec. II. Experimental results of the reactions ^{20}Ne(^{3}He,t)^{20}Na and ^{20}Ne(p,n)^{20}Na including the spin-parity assignments are summarized in sec. III, and the stellar reaction rate is calculated and discussed in sec. IV.

II. EXPERIMENT

The measurement of the differential cross sections of the ^{20}Ne(^{3}He,t)^{20}Na reaction was performed with a 55.33-MeV ^{3}He beam of about 0.5 - 1 μA from the sector-focussing cyclotron of Institute for Nuclear Study, University of Tokyo. A gas target of enriched ^{20}Ne (99.95%) of about 100 mmHg, which has a window of 2.2 μm Havar foil, was used together with a double slit system. The reaction products tritons were measured by using a QDD-type magnetic spectrograph[8] and a hybrid-type position-sensitive gas counter[9] placed on the focal plane. This system provides complete particle identification for tritons by using the energy loss, the total energy and the time-of flight signals. The incident energy was chosen to optimize the energy resolution with the gas target and avoid complexity of the reaction mechanism at low energy although it is still not high enough. There were no deuterons coming in to the focal plane at this energy. The overall energy resolution obtained was about 75 keV. The observed peaks were carefully calibrated by using the known reactions ^{16}O(^{3}He,t)^{16}F and ^{14}N(^{3}He,t)^{14}O. The experimental uncertainties in the excitation energies obtained come mostly from those of the reference peaks of ^{16}F and ^{14}O (10 - 60 keV) and partly due to a possible errors in peak-fitting of overlapped states.

The ^{20}Ne(p,n)^{20}Na reaction was studied by using a 35-MeV proton beam and a high-resolution time-of-flight facility[10] at the Cyclotron-Radioisotope Center of Tohoku University. A beam swinger system was

used in front of the target to measure the differential cross sections at angles of -5 to 150 degrees. A gas target of about 400 mmHg of ^{20}Ne enriched to 99 % was bombarded. The flight path was 44.23 m. The overall time resolution was about 1 ns, and the overall energy resolution was about 80 keV for the most energetic neutrons for this reaction. The uncertainties in excitation energy, however, are due to that of the incident energy and the straggling in the target.

III. EXPERIMENTAL RESULTS

Figure 2 shows a typical momentum spectrum of tritons from the $^{20}Ne(^{3}He,t)^{20}Na$ reaction. There are several states excited above the threshold of p + ^{20}Ne, 2.199 MeV. The levels observed in the (^{3}He,t) and (p,n) reactions on ^{20}Ne are summarized in table 1, together with spin-parity assignments made from the analyses of the angular distributions,

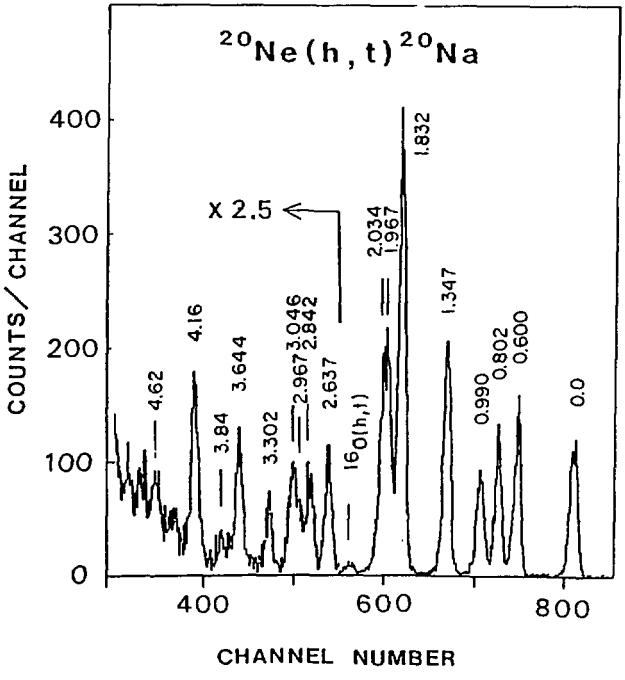

Fig. 2 The triton momentum spectrum from the $^{20}Ne(^{3}He,t)^{20}Na$ reaction at 14° with E_{Lab} = 55.33 MeV.

TABLE 1 Levels of ^{20}Na. Energies are given in MeV.

Adopted J^π	Present (^{3}He,t) Ex	ΔE	J^π	Present (p,n) Ex	ΔE	J^π Ex	Lamm (^{3}He,t) ΔE	
2+	0.0	0.000	(1,2,3)+	0.0	0.000	2+		
3+	0.600	0.015	(3,4,5)+	0.580	0.015	3+		
4+	0.802	0.015	(3,4,5)+	0.790	0.015	4+		
1+	0.990	0.015	(1,2,3)+	0.993	0.015	1+		
2-	1.347	0.015	(2,3,4)-	1.353	0.015	(2-)	1.32	0.02
2-	1.832	0.015	(2,3,4)-	1.843	0.015	(2-)	1.82	0.02
							1.91	0.02
3-	1.967	0.020	(2,3,4)-	2.016	0.020	(3-)	1.98	0.02
(3,4,5)+	2.034	0.020	(3,4,5)+				2.09	0.02
							2.57	0.02
1+	2.637	0.015	(0,1)+	2.651	0.020	1+	2.66	0.02
(3)+	2.842	0.015	(3,4,5)+	2.852	0.020	(2,3)+	2.88	0.04
	2.967	0.020					2.96	0.04
(1,2,3)+	3.046	0.020	(1,2,3)+	3.053	0.020		3.06	0.04
							3.16	0.04
(4,5,6)-	3.302	0.030	(4,5,6)-					
((2,3,4)-)	3.644	0.030	((2,3,4)-)	3.636	0.020			
	3.84	0.040						
(4,5,6)-	4.16	0.040	(4,5,6)-					
	4.62	0.050						
((3,4,5)+)	5.20	0.050	((3,4,5)+)					
(2,3,4)-	5.59	0.060	(2,3,4)-					

which will be discussed later. The first excited state above the threshold is identified at 2.637 MeV[7]. The excitation energies obtained here are consistent with each other with some differences, e.g., the state at 3.302 MeV was not observed in the (p,n) reaction. This is because the state has a high spin of $(4,5,6)^-$. Most states by Lamm et al.[6] also agree within the errors. However, their peaks at 2.57 and 1.91 MeV were not observed in the present experiments. The former peak is possibly due to tritons from oxygen contamination in the gas target since there is a small peak observed at the same position in the present experiment where we have used more isotopically purified ^{20}Ne gas, or due to deuterons as their triton spectrum was severely contaminated with deuterons. For the latter peak at 1.91 MeV, we have not seen at the energy consistently a peak at 16 angles, where they claimed a state by measurements at four angles.

Angular distributions were measured for both the (^{3}He,t) and (p,n) reactions on ^{20}Ne. Figures 3 and 4 show the angular distributions of the (^{3}He,t) and (p,n) reactions, respectively. All angular distributions of the (^{3}He,t) reaction have oscillatory patterns. Especially, the first and the second peak angles are shown to be characteristic to the transferred angular momentum (L), but not to other quantum numbers like the transferred spin (S) and transferred total spin (J), and also to the shell

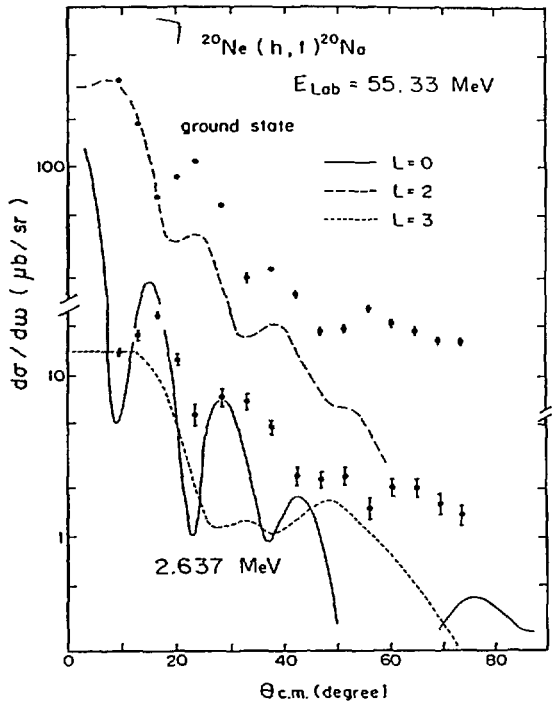

Fig. 3 The angular distributions of the reaction $^{20}Ne(^3He,t)^{20}Na$ for the ground state and the 2.637 MeV state. The solid line is the DWBA calculation assuming $(s_{1/2}s_{1/2}^{-1})_{S=0,\ L=0,\ J=0}$, the dotted line $(d_{5/2}p_{1/2}^{-1})_{S=0,\ L=3,\ J=3}$, and the dashed line $(d_{5/2}d_{5/2}^{-1})_{S=0,\ L=2,\ J=2}$.

model configurations assumed. On the other hand, the (p,n) reactions at 35 MeV are known to have angular distribution shapes characteristic to the transferred total angular momentum (J), and also to the shell model configurations[11]. The (p,n) reactions predominantly go through one-step process with $(\sigma\tau)$ and exchange interactions. Further, they more or less excite collective states like 1^+ states, but not 0^+ states. Thus, the (p,n) reaction can be used complementary to the (^{3}He,t) reaction for nuclear spectroscopy. These features were well confirmed by Distorted-Wave Born Approximation (DWBA) calculations and second-order DWBA calculations.

To determine the spin-parity of each state DWBA calculations have been performed for both (^{3}He,t) and (p,n) reactions. For the (^{3}He,t) reactions an effective interaction of Shaeffer[12] was used for the reaction

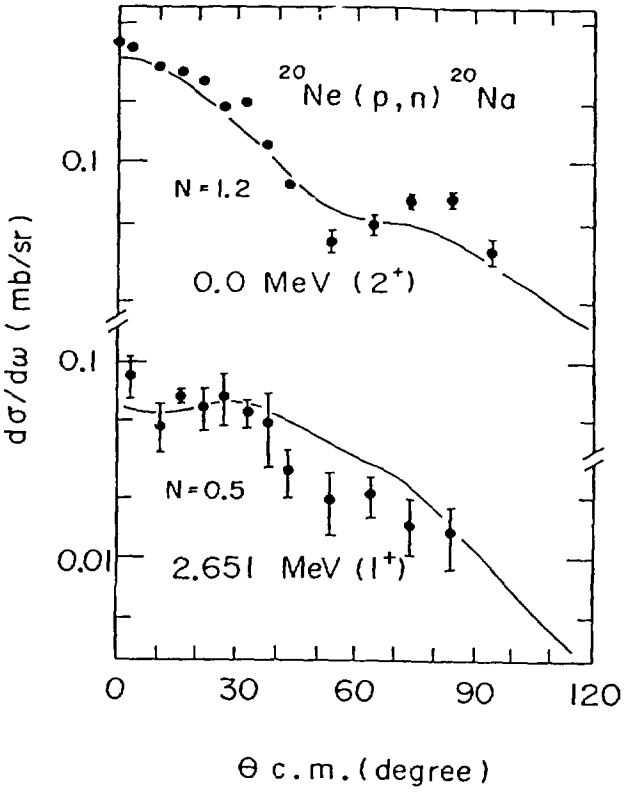

Fig. 4 The angular distributions of neutrons from the $^{20}Ne(p,n)^{20}Na$ reaction for the ground state and the 2.651 MeV state at E_{Lab}=35 MeV. N is the normalization factor for the DWBA calculation to fit the data.

interaction. The unbound single particle states were generated by assuming a slight binding of 0.1 MeV. These usually do not affect much to the shapes of the (^{3}He,t) angular distributions. The optical potential parameters for ^{3}He were obtained by optical model analysis of the elastic scattering data measured here in the same experimental setups, and those for the triton channel were assumed to be the same as the ^{3}He channel. The proton optical potential was that of Becchetti and Greenlees[13], and that for the neutron was of Carlson et al.[14].

At forward angles, the peak angles of the (^{3}He,t) angular distribution for the ground state are well reproduced by the DWBA calculation with L = 2, as can be seen in Fig. 3. Ths is consistent with that this state has 2^+.

Here, no fitting to the shapes was tried by modifying the parameters. Similarly, the peak angles of the angular distribution for the 2.637-MeV state also are reproduced by the calculation of L = 0, although there are some discrepancy at large angles. This is due to the unresolved peak of the $^{16}O(^3He,t)$ reaction of L = 3 at large angles. However, the angles of the first two peaks and the strong oscillations are very much characteristic to L = 0 transition. Thus, this state should have either $J^\pi = 0^+$ or 1^+. On the other hand, the (p,n) reaction excites this state with considerable intensity. This facts suggest that this state to be 1^+ rather than 0^+ as discussed above. Actually, the DWBA calculation with J = 1 reproduces the angular distribution very well. Fig. 4 shows the angular distribution for the state together with a DWBA calculation of J = 1 assuming the wave function obtained with a full $(d_{5/2}s_{1/2}d_{3/2})$ space shell model calculation by Brown and Wildenthal[15]. The transition density by the shell model for this state is $0.281(\pi s_{1/2}\nu s_{1/2}^{-1})$ - $0.154(\pi d_{5/2}\nu d_{5/2}^{-1})$ + $0.147(\pi d_{3/2}\nu d_{5/2}^{-1})$ + $0.124(\pi d_{5/2}\nu d_{3/2}^{-1})$, where the $s_{1/2}$ component dominates the transition. This should be compared with the 0.99-MeV 1^+ state, which has the dominant component of $d_{5/2}$ and $d_{3/2}$. The normalization factor needed to fit the data is quite reasonable, N = 0.5. Note that if the level assignment is wrong, one usually gets a large deviation from unity in the (p,n) reaction at this energy. From the analysis of both $(^3He,t)$ and (p,n) reactions, it is concluded that this state has $J^\pi = 1^+$ with a large $s_{1/2}$ component.

Adopted spin-parity assignments here are summarized in table 1 together with those made by each reaction. Figure 4 includes the normalization factors (N) needed to fit the data with the DWBA calculations using the shell model wave functions. The normalization factors for other states also seem to be reasonable as they do not deviate much from unity. The levels observed here correspond well to the states in ^{20}F up to around 3.5 MeV. The trend of the Coulomb shifts from ^{20}F was well predicted by Langanke et al.[3]. However, they predicted the 3^- state at 2.856 MeV to be the first excited state above the threshold in ^{20}Na, and the 1^+ state at 2.876 MeV, which can be the s-wave resonance in the p + ^{19}Ne scattering.

IV. STELLAR REACTION RATE OF THE $^{19}Ne(p,\gamma)^{20}Na$ PROCESS

The $^{19}Ne(p,\gamma)^{20}Na$ and $^{15}O(\alpha,\gamma)^{19}Ne$ reactions are the key reactions which determine the rate of breakout off the HCNO cycle and the following synthesis of heavy elements[1], as shown in Fig. 1. Here, we have evaluated the stellar reaction rate of the $^{19}Ne(p,\gamma)^{20}Na$ process at stellar

temperature $0.1 < T_9 < 2.0$, where $T_9 = T/10^9$ K, in novae or accreting white dwarfs. The HCNO cycle is presumed to take place in these stellar objects.

The stellar reaction rate consists of three parts,

$$N_A\langle\sigma v\rangle = N_A\langle\sigma v\rangle_R + N_A\langle\sigma v\rangle_{TAIL} + N_A\langle\sigma v\rangle_{DC}, \quad (1)$$

where $\langle\sigma v\rangle$ is a thermally averaged reaction rate, σ is the total reaction rate, and N_A is the Avogadro number. The first term denotes the resonant contribution to be discussed in this section, the second is that from the low-energy tails of the resonances, and the third is the direct capture contribution. The second and third terms are taken from the previous theoretical estimates[3,16,17]. The first resonant term in unit of cm^3/sec./gr·mole is written as

$$N_A\langle\sigma v\rangle = 1.65\times10^5\, T_9^{-3/2}\Sigma_r\omega_r \exp(-11.605E_r/T_9), \quad (2)$$

where E_r is the resonance energy in MeV, and ω_r is the resonance strength in eV defined by

$$\omega_r = (2J + 1)/4 \cdot \Gamma_p\Gamma_\gamma/\Gamma_{tot}. \quad (3)$$

Here, J is the total angular momentum of the resonance, $\Gamma_{tot} = \Gamma_p + \Gamma_\gamma$, and Γ_p and Γ_γ are the gamma and proton widths, respectively. The adopted resonance parameters are summarized in table 2. The resonance energies and the spin-parities of the first two states in the table are taken from the present experiment, and the others from ref. 3). The gamma widths are simply assumed to be the same as those in ^{20}F, and the proton widths were taken from the recent reevaluation by Langanke et al.[3] because of lack of the experimental data. We believe that this parametrization is

TABLE 2 Resonance parameters for the ^{19}Ne(p,γ) process.

Excitation Energy	Ex. - Threshold	J^π	l	θ_p^2	Γ_p (eV)	Γ_γ (eV)	$\omega\gamma$ (eV)
2.637	0.438	1+	0	0.4	6800.0	0.015	0.0113
2.842	0.643	3+	2	0.054	11.3	0.011	0.0192
2.856*	0.657	3 -	3	0.006	0.029	0.038	0.0288
2.996*	0.797	1+	0	0.08	3200.0	0.016	0.012

* Taken from ref. 3).

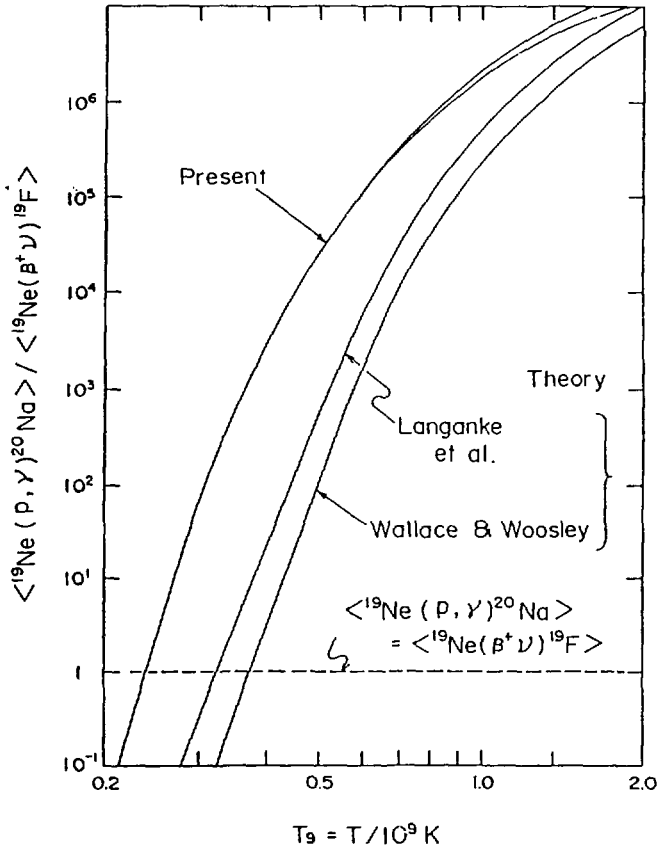

Fig. 5 Calculated stellar reaction rate based on the present experimental results, and theoretical predictions by Wallace and Woosley[1], and Langanke et al.[3]. All calculations are plotted in unit of the β-decay rate of ^{19}Ne(g.s.) (β^+ ν) ^{19}F(g.s.).

appropriate (at the risk of the two assumptions above on ω_r) in order to see the effects of the low-lying resonances which were found experimentally for the first time in the present experiment. The proton reduced widths were taken from the analogue states in ^{20}Ne.

The calculated stellar reaction rate is displayed in Fig. 5 together with previous theoretical estimates[1,3]. The present result is about two orders of magnitude larger than the prediction by Langanke et al.[3] at $0.3 < T_9 < 0.5$, but very close to theirs at very low temperatures. This is because the direct capture contribution dominates the reaction rate at $E_{c.m.} < 0.4$ MeV,

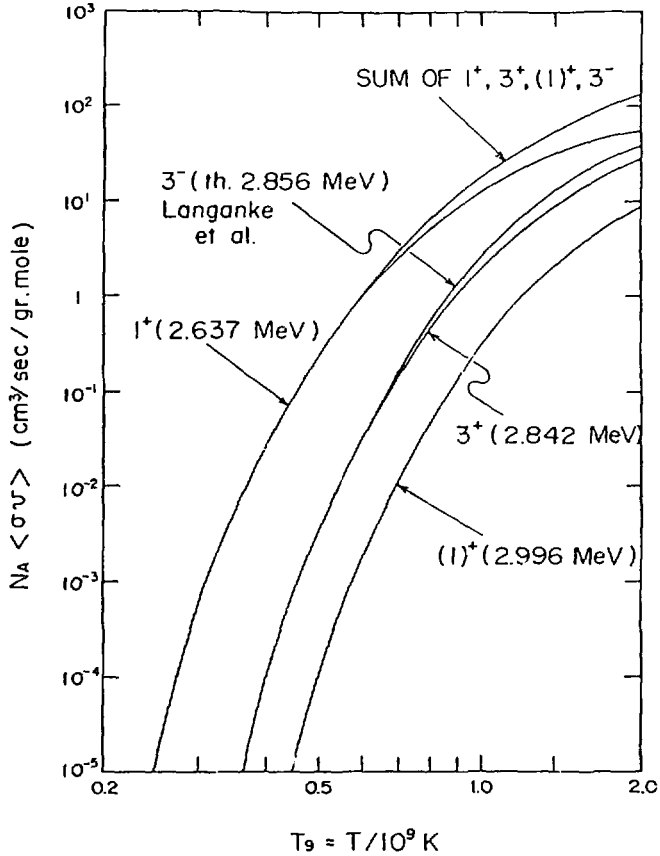

Fig. 6 The present calculated stellar reaction rates for each resonances denoted. The parameters for the 3^- state were taken from ref. 3).

as was pointed out in ref. 3), and the present calculation assumes the same function for this contribution. However, the resonance contribution progressively dominates the rate, specifically the 1^+ (2.637 MeV) and 3^+ (2.842 MeV) states enhance the reaction rate of the proton captures at higher temperatures, as shown in Fig. 6. The other resonances have smaller contributions by an order of magnitude or more at $0.1 < T_9 < 1.0$.

Figure 5 shows the relative ratio of the calculated reaction rate $N_A\langle\sigma v\rangle$ for $^{19}Ne(p,\gamma)^{20}Na$ to the beta decay rate of $^{19}Ne(\beta^+\nu)^{19}F$

$$R = \rho N_A\langle\sigma v\rangle/(ln2/\tau_{1/2}), \qquad (4)$$

assuming the typical density $\rho = 5 \times 10^5$ gr·mole/cm^3 of novae. The proton capture process dominates over the β-decay for a wide range of temperature of interest. The reaction rate exceeds the β-decay rate already at around $T_9 = 0.23$. This critical temperature is much lower than the previous theoretical prediction $T_9 = 0.3 - 0.4$[1,3]. This can be considered to be the breakout temperature from the HCNO cycle since other processes rather than the $^{15}O(\alpha,\gamma)^{19}Ne$ reaction are also possible to reach ^{19}Ne already at $T_9 = 0.2$ as pointed out by Wiescher et al.[2]. Therefore, this critical temperature suggests that the CNO materials are easily transformed into Ne-Na isotopes and build up heavier elements in the rp-process[1] when the stellar temperature goes over $T_9 = 0.23$.

Although no 3^- and the third 1^+ states were observed above the proton threshold in the present experiment, we have included the contributions to eq. (2) by adopting the same parameter set as in ref. 2). The result is shown in Fig. 5. The inclusion of 3^- and 1^+_3 states do not change so much the total reaction rate below $T_9 = 0.6$. Thus, the strong enhancement of the reaction rate at the temperature of interest is mainly due to the 1^+ (2.637 MeV) state, and the breakout temperature $T_9 = 0.23$ from the HCNO cycle remains unchanged.

V. CONCLUSION

The level structure of ^{20}Na has been studied experimentally by using the (^{3}He,t) and (p,n) reactions on ^{20}Ne. The spin-parities have been determined for the first time for the states near and above the p + ^{19}Ne threshold. The excitation energies of the states also have been determined by the two reactions. Specifically, the first excited state above the threshold has been identified to be $J^\pi = 1^+$ at 2.637 MeV with a large $s_{1/2}$ component.

The stellar reaction rate of the $^{19}Ne(p,\gamma)$ process has been evaluated based on the present experimental data. The calculation shows more than two orders of magnitude larger rate than the previous theoretical predictions. The onset temperature of the breakout from the HCNO cycle is found to be about $T_9 = 0.23$. The present finding of the s-wave resonance just above the capture threshold possibly explains the strong enhancement of Ne and heavier elements in nova observations, and change possibly the onset temperature of the rp-process as well.

REFERENCES

1) R. H. Wallace, and S. E. Woosley, Astrophys. J. Suppl. 45 (1981) 389.
2) M. Wiescher, J. Gorres, F. -K. Thielemannn, and H. Ritter, Astron. Astrophys. 160 (1986) 56.
3) K. H. Langanke, M. Wiescher, W. A. Fowler, and J. Gorres, Astrophys. J. 301 (1986) 639.
4) F. Ajzenberg-Selove, Nucl. Phys. A475 (1987) 1.
5) J. Aysto, et al., Phys. Rev. C23 (1981) 879.
6) L. O. Lamm, C. P. Browne, J. Gorres, M. Wiescher, and A. A. Rollefson, Z. Phys. A327 (1987) 239.
7) S. Kubono, et al., Z. Phys. A (1988) (in press).
8) S. Kato, M. Tanaka, and T. Hasegawa, Nucl. Instr. Meth. 154 (1978) 19.
9) M. H. Tanaka, S. Kubono, and S. Kato, Nucl. Instr. Meth. 195 (1982) 509.
10) H. Orihara and T. Murakami, Nucl. Instr. Meth. 188 (1981) 15.
11) K. Furukawa, et al., Phys. Rev. C36 (1987) 1986.
12) R. Shaeffer, Nucl. Phys. A164 (1971) 145.
13) F. D. Becchetti, Jr. and G. W. Greenlees, Phys. Rev. 192 (1969) 1190.
14) J. D. Carlson, C. D. Zafiratos, and D. A. Lind, Nucl. Phys. A249 (1975) 29.
15) B. A. Brown and B. H. Wildenthal (1988), unpublished.
16) W. A. Fowler, G. R. Caughlan, and B. A. Zimmerman, Ann. Rev. Astron. Astrophys. 5 (1967) 525 and 13 (1975) 69.
17) C. Rolfs, Nucl. Phys. A217 (1973) 29.